J. Braz. Chem. Soc., Vol. 21, No. 7, 1359-1365, 2010.
Printed in Brazil - ©2010 Sociedade Brasileira de Química
0103 - 5053 $6.00+0.00

Article

Growth of TiO_2 Nanotube Arrays with Simultaneous Au Nanoparticles Impregnation: Photocatalysts for Hydrogen Production

Adriano F. Feil,[a] Pedro Migowski,[b] Francine R. Scheffer,[b] Matheus D. Pierozan,[a] Rodrigo R. Corsetti,[a] Melissa Rodrigues,[b] Rafael P. Pezzi,[b] Giovanna Machado,[c] Livio Amaral,[a] Sérgio R. Teixeira,*[,a] Daniel E. Weibel*[,b] and Jairton Dupont*[,b]

[a]Instituto de Física and [b]Instituto de Química, Universidade Federal do Rio Grande do Sul, UFRGS, Av. Bento Gonçalves, 9500, 91501-970 Porto Alegre-RS, Brazil

[c]CCET, Universidade de Caxias do Sul, Rua Francisco Getúlio Vargas, 1130, 95070-560 Caxias do Sul-RS, Brazil and Centro de Tecnologia Estratégicas do Nordeste, CETENE, Av. Prof. Luiz Freire, 01 - Cidade Universitária, 50740-540 Recife-PE, Brazil

Um novo método para a fabricação de nanotubos (NTs) de TiO_2 organizados e impregnados com nanopartículas (NPs) de ouro foi desenvolvido, e as propriedades estruturais, morfológicas e ópticas dos NTs obtidos foram investigadas. Os arranjos de NTs de TiO_2 foram crescidos pela oxidação anódica de Ti metálico utilizando soluções eletrolíticas contendo íons fluoreto e NPs de Au. As estruturas resultantes foram caracterizadas por espectrometria de retroespalhamento Rutherford (RBS), difratometria de raios X com incidência rasante (GIXRD), microscopias eletrônicas de transmissão (TEM) e de varredura (SEM) e espectroscopia UV-Vis. Tanto os arranjos de NTs sem Au quanto os impregnados com Au mostraram atividade fotocatalítica boa e estável na geração de hidrogênio a partir de misturas água/metanol. Os nanotubos de TiO_2 contendo Au foram mais ativos na fotogeração de hidrogênio do que os NTs de TiO_2 sem Au.

A novel method for the fabrication of TiO_2 nanotubes (NTs) impregnated with gold nanoparticles (NPs) is reported. TiO_2 NT arrays were grown by anodic oxidation of Ti metal using fluoride electrolytes containing Au NPs. Resulting structures were characterized by Rutherford backscattering spectrometry (RBS), grazing incidence X-ray diffractometry (GIXRD), transmission and scanning electron microscopy (SEM and TEM) and UV-Vis spectroscopy. Au-free and Au-impregnated TiO_2 NT arrays showed good and stable photocatalytic activity for hydrogen generation from water/methanol solutions. Au-containing TiO_2 NTs presented higher hydrogen photogeneration activity than Au-free TiO_2 NTs.

Keywords: water splitting, hydrogen production, photocatalysis, titanium dioxide nanotubes, nanoparticles

Introduction

Given the growing demand for environmentally friendly energy generation from renewable sources, intensive efforts have been directed to research and development of solar energy conversion materials. Furthermore, the intermittent nature of solar radiation incident on Earth's surface due to the day/night cycle and variable atmospheric conditions demands a reliable method for energy storage and transport, so that the energy may be conveniently utilized on demand.

One of the most promising forms of clean energy generation and storage involves molecular hydrogen. Hydrogen can be used for electricity generation in fuel cells or in combustion engines, with water being the only byproduct. However, finding an environmentally friendly source of hydrogen gas is still an important challenge, since the current industrial processes for H_2 generation are still dependent on fossil fuels[1] and, consequently, generate huge amounts of greenhouse gases. In this scenario, the photocatalytic splitting of water into O_2 and H_2 is an interesting alternative.

It has been shown that wide band-gap materials such as titanium dioxide (TiO_2) can be used for photocatalytic water splitting under solar radiation.[2] Moreover, due to

*e-mail: jairton.dupont@ufrgs.br
Dedicated to Prof. Ícaro de Sousa Moreira for his contribution to Bio-Inorganic Chemistry in Brazil

its relatively low cost and chemical and photo stability, TiO_2 has been recognized as a promising material for photochemical applications.[3]

Among the various methods available for the preparation of TiO_2 nanomaterials,[4] the syntheses of TiO_2 nanotubes (NTs) through the anodization of metallic Ti surfaces has several advantages.[5,6] The main benefits are a simple synthetic procedure, enhanced charge transport properties and a cost-effective scale-up process.[7] In addition, self-organized TiO_2 NT arrays grown by anodization processes present enhanced photocatalytic activity when compared to randomly-oriented nanoparticles (NPs) or nanotubes prepared by other methods such as the sol-gel (hydrothermal) process.[7,8]

One of the biggest limitations of TiO_2 is its relatively large band gap between 3.0 and 3.2 eV.[9] Therefore, only UV light can be utilized for hydrogen production. Since UV light only accounts for about 5% of the solar radiation that reaches Earth's surface, the inability to utilize visible light limits the efficiency of solar photocatalytic hydrogen generation. Thus, different strategies have been adopted in order to improve this efficiency, including: *i*) varying the sizes of the nanoparticles,[10] *ii*) doping with metal/non-metal ions,[11] *iii*) coupling the titanium dioxide with low band gap semiconductors,[12] and *iv*) supporting metallic/metal oxide nanoparticles on the oxide surface to promote electron and hole transfer reactions at the TiO_2/substrate interface.[13,14] In addition, it is desirable to produce TiO_2 structures composed mainly of the anatase phase, because it has higher catalytic activity than the rutile phase.[3]

In general, anodic TiO_2 NTs photocatalytic activity enhancement is also achieved by metal/non-metal ion doping, sensitization with lower band gap semiconductors and supported metal NPs. Ionic doping could be performed by choosing the appropriate electrolyte solution[15,16] (especially for anionic doping), performing the thermal annealing crystallization,[17] anodizing metal alloys,[18,19] or by ion implantation.[20,21] Other methods involve impregnation of pre-formed materials.[22,23] For example, TiO_2 nanotube arrays were prepared by anodization and then impregnated with thiol-passivated quantum dots for solar cell applications.[23]

Herein we describe a novel fabrication method for the growth of TiO_2 NT arrays with simultaneous metal nanoparticle impregnation during anodic oxidation. The nanotube arrays prepared in the presence of metal nanoparticles were characterized by scanning and transmission electron microscopy (SEM and TEM, respectively) and Rutherford backscattering spectrometry (RBS). Structural and optical characteristics were assessed by grazing incidence X-ray diffraction (GIXRD) and UV-Vis spectroscopy analyses. The photocatalytic activity of the synthesized NTs for hydrogen generation was also evaluated for Au-free and Au-impregnated arrays.

Experimental

Materials and methods

All chemicals were purchased from commercial sources: tetrachloroauric(III) acid hydrate ($HAuCl_4 \cdot H_2O$, 99.9%) and sodium citrate dihydrate (99%) from Strem Chemicals, NH_4F (98%), ethylene glycol 99% (ETG) and Ti foil (99.6%) from Synth. Solvents and reagents were used as received.

The nanostructures were characterized by SEM, TEM, GIXRD, UV-Vis spectroscopy and RBS. Electronic microscopy images were obtained with a JEOL 6060 SEM and a JEOL JEM 1200ExII TEM. Chemical analyses by line scans and mapping were performed with an electron probe energy dispersive X-ray spectrometer (EDX) in scanning field emission gun (FEG) mode. Transmission and diffuse reflectance UV-Vis spectra were recorded on a Cary-100 spectrophotometer. GIXRD patterns were recorded at the Laboratório Nacional de Luz Síncrotron (LNLS, XRD-2 beam line, λ = 1.50 Å, Campinas, Brazil). RBS analyses were conducted using alpha particles accelerated to 1 MeV (normal incidence and 15° detection), allowing the quantification of the gold present in the nanotubes and providing an approximate Au depth profile. Au quantification was carried out by comparison with a standard reference that consisted of an Au-free TiO_2 NTs array implanted with 1×10^{16} Au atoms cm^{-2}.

Gas chromatography analyses were conducted on an Agilent 6820 GC chromatograph equipped with a thermal conductivity detector (TCD). A Porapak-Q packed column was used with argon as carrier gas.

Synthesis of Au nanoparticles

The gold nanoparticles were synthesized by a slight modification of the classical citrate method.[24] Three different Au NPs concentrations were attained from a 5×10^{-3} mol L^{-1} stock solution (SS) of $HAuCl_4$ as follows: 2.6×10^{-4} mol L^{-1} (1 mL of SS diluted with 18 mL of deionized water, DW); 16×10^{-4} mol L^{-1} (5 mL SS + 10 mL DW) and 50×10^{-4} mol L^{-1} (10 mL of undiluted SS). Each solution was heated to boiling and then received the addition of an equal volume of a 2×10^{-2} mol L^{-1} sodium citrate solution. All colloids prepared by this method were imaged by TEM and their size distributions were determined by counting a minimum of 300 particles.

TiO_2 nanotube array synthesis

Au-free and Au-impregnated NT arrays were synthesized by electrochemical anodization of Ti foil in fluoride-containing ethylene glycol (ETG) electrolytes.[25] Au-free titanium dioxide NTs were formed by anodizing 1.23 cm^2 of a Ti foil (applied electrical potential 20 V) for 2 h in an ultrasonic bath. In this case, ETG solutions containing 0.25 wt.% NH_4F and 10 wt.% water were employed. In order to impregnate the NTs with Au NPs, the electrochemical anodization of Ti foil in fluoride-containing ETG electrolytes was conducted using 10 wt.% Au NPs solution prepared as described in the preceding section, starting from different initial $HAuCl_4$ concentrations. After the anodization process, the TiO_2 films were rinsed with water and dried under N_2 flux. Dried nanotubes were thermally annealed at 400 or 580 °C for 3 h in air in order to crystallize the oxide film.

Photocatalytic H_2 generation

Hydrogen photogeneration experiments were carried out in a calibrated, gas-closed photochemical reactor made of polytetrafluoroethylene (PTFE) under continuous magnetic stirring. A quartz window allowed irradiation of the aqueous mixture under a wide incident spectral range, including UV and visible light. A 150 W mercury-xenon lamp (Sciencetech Inc.) operating at about 78% power was used as excitation source. The light beam was focused to cover homogeneously the whole photocalyst surface (1.23 cm^2). TiO_2 NTs were placed in a special PTFE support to avoid photocatalytic activity in regions other than the NTs. Prior to irradiation, the reactor was deaerated with argon by using custom-made PTFE valves. The photocatalytic activity of the titania NTs was evaluated by gas chromatography, measuring the hydrogen production at room temperature from a mixture of water/methanol (8/1, v/v). A maximum volume of 500 µL of the gas contained in the closed reactor was collected with a gas-tight syringe, and the amount of hydrogen produced was measured in hourly intervals.

Results and Discussion

All gold colloids prepared by citrate reduction of aqueous solutions of $HAuCl_4$ showed spherical NPs with the same average diameters (12.2 ± 2.8 nm), Figure 1(a-c). When dispersed in NH_4F/ETG solutions, the color of the colloids changed from red to blue (Supplementary Information, Figure S1). These color changes are due to NP agglomeration, as can be observed in the TEM images of Figure 1(d-f). Besides the agglomeration, there were no changes in the shape and size of gold nanoparticles in the ETG electrolyte solutions. It is important to point out that the anodization must be effective under ultrasonic conditions to avoid precipitation of the nanoparticles during NT growth.

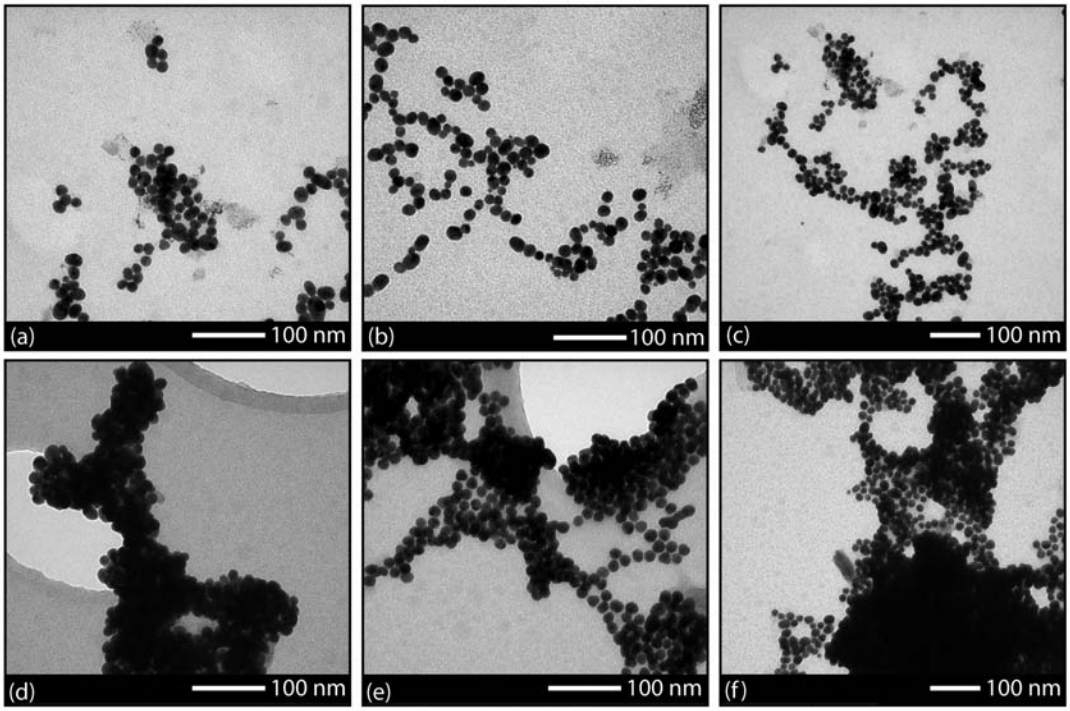

Figure 1. TEM images of (a-c) Au NPs prepared with different initial $HAuCl_4$ concentrations, and (d-f) ETG/NH_4F electrolytes containing the respective Au NPs.

Figure 2(a,b) presents surface and cross-section SEM micrographs of Au-free TiO_2 NT arrays. The images show that TiO_2 NTs are 1.5 μm long with external and internal diameters of 60 nm and 40 nm, respectively. Figure 2(c,d) shows Au chemical mapping of the surface and cross-section of the NTs structure as obtained by SEM-EDX from TiO_2 NTs grown in Au NPs-containing electrolytes. Both anodization procedures generated TiO_2 with the same morphological characteristics, showing that the Au NPs do not affect the growth of the NTs. On the other hand, Figure 2d also shows a higher concentration of Au at the top of the NTs than along the tubular structure.

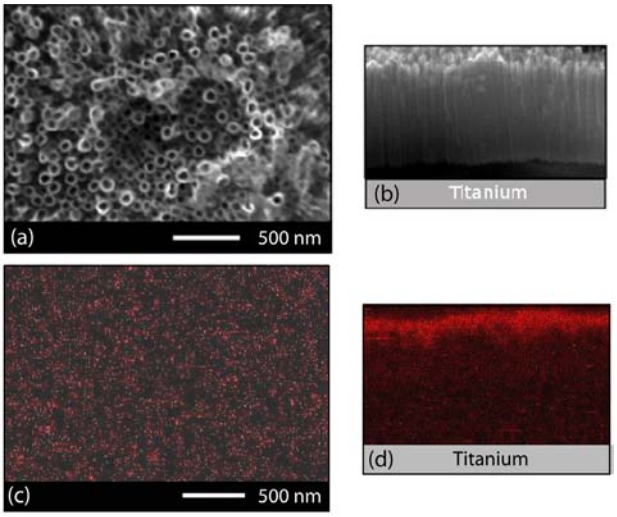

Figure 2. Top view (a) and cross-section (b) SEM images of a typical Au-free TiO_2 nanotube array grown in an ETG/ammonium fluoride solution. Top view (c) and cross-section (d) Au EDX chemical mapping images of Au-impregnated TiO_2 NTs.

To get more detailed information about the actual Au distribution in the Au-impregnated TiO_2 NTs, RBS analysis was carried out. Figure 3 shows the results for the three Au concentrations used. RBS spectra corroborate the microscopy results (see SEM EDX images in Figure 2d) and also indicate that Au is heterogeneously distributed along the length of the NTs. The Au concentration near the top of the NTs arrays is significantly higher (as indicated by the arrow) than in the regions near the titanium substrate. RBS data also enabled the quantitative determination of the amount of gold present in the gold-impregnated samples. The amount of Au introduced in the TiO_2 NTs increased when higher concentrations of Au NPs were used in the electrolyte solutions. The results are summarized in Table 1.

It is known that the growth of TiO_2 nanotubes by anodization processes typically results in amorphous structures, and that anatase and/or rutile phases are formed after thermal annealing.[26] The fcc diffraction pattern

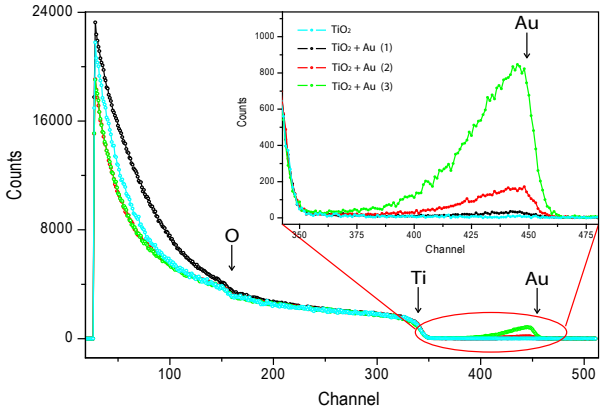

Figure 3. RBS spectra of Au-impregnated TiO_2 NTs. The inset shows the region corresponding to ions scattered from Au atoms present on the NTs.

Table 1. Concentrations of gold in impregnated TiO_2 NTs determined by RBS as a function of Au NPs concentration

TiO_2+Au system	Concentration of the Au NPs solutions added to the ETG electrolyte (mol L^{-1})	Amount of gold impregnated on TiO_2 NTs (atoms cm^{-2})
1	2.5×10^{-4}	5.56×10^{14}
2	13×10^{-4}	1.86×10^{15}
3	25×10^{-4}	8.34×10^{15}

of gold structures is difficult to visualize in crystalized TiO_2, since its intensity is very low due to the inherent nanometric size and low concentration compared with TiO_2 structures. Additionally, the major diffraction peaks of the fcc gold structure match those from crystalline TiO_2 phases. However, in the non-annealed samples, Figure 4a, the presence of Au in the TiO_2 NT arrays can be observed. Figure 4 also shows a comparison of the GIXRD patterns of crystalized TiO_2 nanotube structures in its Au-free and

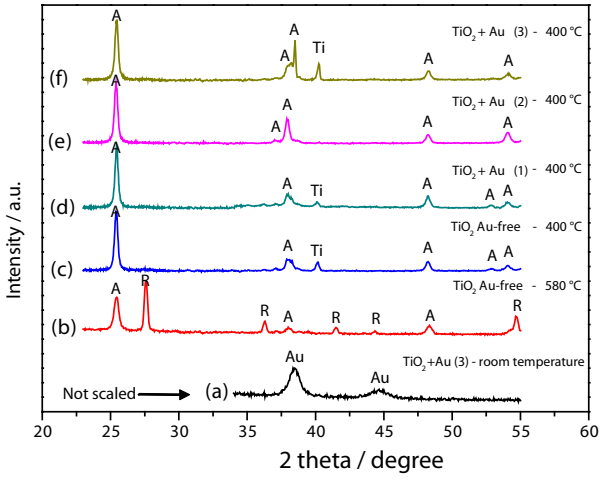

Figure 4. GIXRD patterns of Au-free and Au-impregnated TiO_2 nanotubes after thermal treatment under different temperatures. A, R, Ti and Au represent anatase, rutile, titanium and gold diffraction peaks, respectively.

impregnated forms with different Au concentrations after 3 h of annealing in air.

The annealing temperature plays an important role in the phase behavior of TiO_2. The thermal treatment of Au-free NTs at 400 °C generates only the anatase phase, Figure 4c, while at 580 °C 60% of the material is composed by rutile and 40% of anatase, Figure 4b. Since anatase is the desired phase for photocatalytic applications due to its higher activity, all Au-impregnated samples were annealed at 400 °C. As can be seen in Figure 4(d-f), the incorporation of nanoparticles in the NTs structure did not modify the phase behavior at 400 °C, leading to anatase TiO_2 in all cases studied.

The optical properties of the synthesized TiO_2 NTs were investigated by UV-Vis spectroscopy. Figure 5 shows the corresponding spectra of crystallized, pure and Au-impregnate TiO_2 NTs after 3 h of annealing. Figure 5-top shows an intense absorption band between 200 and 400 nm, which is typical of crystalline semiconducting TiO_2. In addition, the structures grown in Au NP-containing solutions presented an absorption component between 500 and 700 nm (see Figure 5-bottom). This band, which corresponds to the plasmon resonance of gold

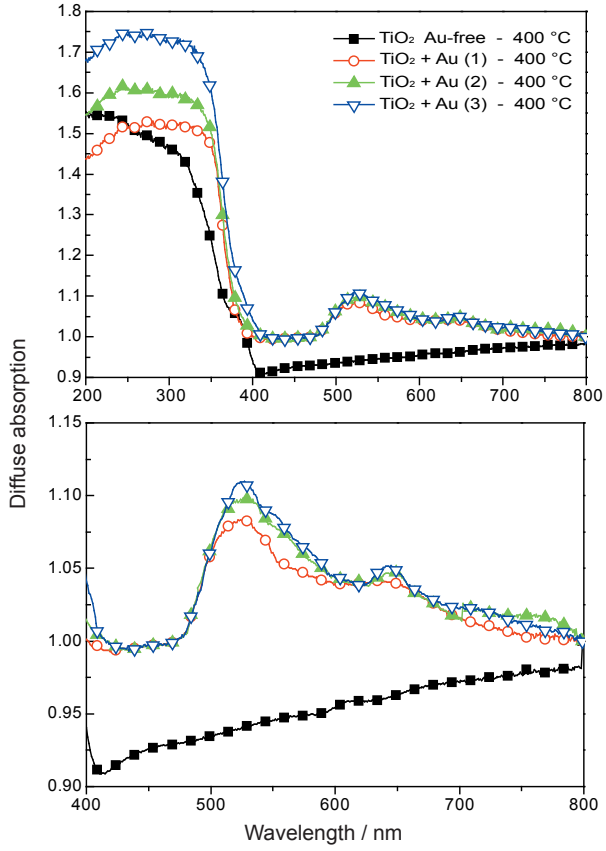

Figure 5. Diffuse UV-Vis absorption spectra corresponding to anodic TiO_2 nanotubes grown from different Au concentrations. Bottom: zoom in the 400-800 nm region.

nanoparticles,[27] is another indication of the presence of Au NPs in the TiO_2 NT arrays.

Photochemical hydrogen generation

Water-splitting reactions using metal oxide semiconductors as catalysts are usually carried out in aqueous solutions with the addition of easily oxidizable reducing agents.[28] The photogenerated holes irreversibly oxidize those agents, such as methanol, instead of water. This effect increases the electron concentration in the photocatalysts, and the hydrogen evolution reaction is enhanced. Reactions using sacrificial agents are regarded as half reactions and are often employed in tests of photocatalytic hydrogen or oxygen evolution. The prepared TiO_2 and Au-impregnated TiO_2 NT arrays were tested for their ability to photochemically split water in a mixture of water and methanol. Figure 6 shows the amounts of hydrogen evolution for pure and Au-impregnated TiO_2 NTs under UV-Vis irradiation. Under dark conditions, no formation of hydrogen was detected on both types of TiO_2 NTs. All nanotube systems showed a linear increase in the amount of hydrogen produced *versus* the UV irradiation time, Figure 6. The rate of hydrogen evolution from Au-free TiO_2 NTs with a phase composition of 60% rutile and 40% anatase was 0.51 μmol cm^{-2} h^{-1}. Hydrogen evolution rate from 100% anatase NTs was 3.5 times higher than with 40% anatase. Impregnation of TiO_2 NTs with Au increased in some cases the hydrogen generation rate. The (TiO_2+Au) NT systems 1 and 2 produced 1.3 and 1.1 times more hydrogen than Au-free NTs. These results suggest that Au-impregnated NTs have higher photocatalytic activity than Au-free TiO_2 nanostructures (100 and 40% anatase phase) under the same illumination conditions. These results can be understood by taking into account the GIXRD data shown in Figure 4. The presence of gold led, in the three Au concentrations studied, to TiO_2 NTs with 100% of anatase phase. The presence of 100% anatase in TiO_2+Au samples guarantees hydrogen generation rates similar to those given by Au-free anatase TiO_2 NTs. However, Figure 6 shows that the hydrogen evolution rate also depends on the Au concentration. As the concentration of gold increases, the hydrogen generation rate decreases, giving almost the same rate as the 100% anatase phase in TiO_2+Au system 3.

As can be seen in Figures 2d and 3, the top region of the NTs has a higher Au concentration, which may decrease the number of active sites proportionally, and therefore decrease the photocatalytic activity of the TiO_2 nanotubes as the Au concentration increases. This is a known effect observed in TiO_2-supported noble metal photocatalysts.[29] Interestingly, with the lowest concentration of Au used,

there was a 1.3 fold increase in the hydrogen evolution rate, in spite of the Au accumulation at the photocatalysts surface. Decreasing even more the concentration of Au would avoid its high accumulation at the surface, leaving more active sites for hydrogen generation. Further experiments in this direction are currently underway and results will be published elsewhere.

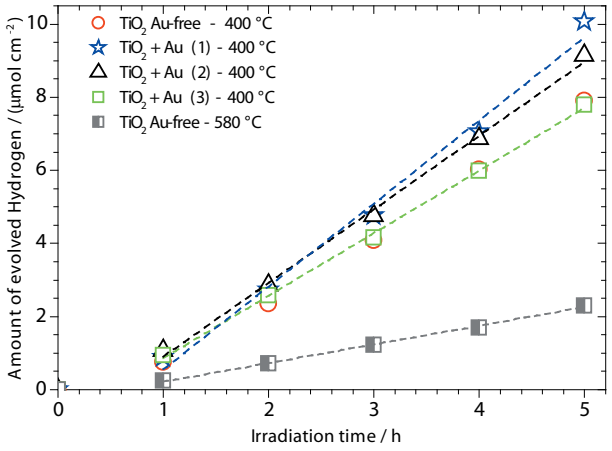

Figure 6. Photocatalytically evolved H_2 from water/methanol (MeOH as electron donor) on pure and Au-doped TiO_2 nanotubes. Water/methanol ratio: 8/1 (v/v).

Since pure and Au-impregnated TiO_2 NTs produced hydrogen under illumination conditions, another important issue to test prior to a successful application was the hydrogen generation stability.

Figure 7 shows a typical time evolution pattern of hydrogen generation from a mixture of water and methanol under UV-Vis illumination using Au-impregnated TiO_2 NTs (system 1). Hydrogen production evolved steadily and the photocatalytic activity did not deteriorate, even after 24 h of continuous irradiation. The same stability in hydrogen evolution rate was observed in Au-free TiO_2 nanotubes, but with lower hydrogen production efficiency.

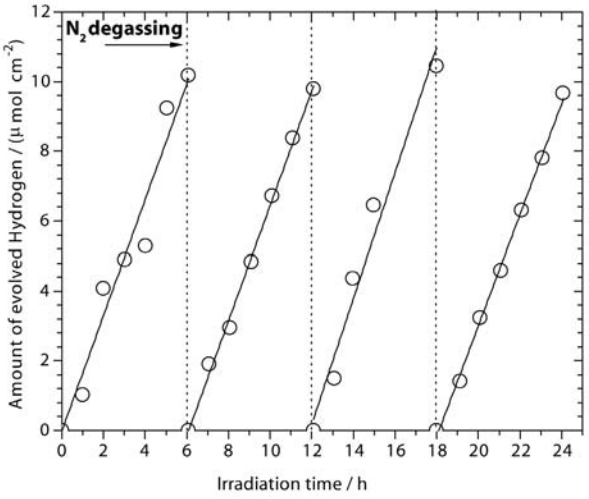

Figure 7. Typical hydrogen evolution rate showing the stability of the photocatalytic reaction. Photocatalyst: Au-impregnated TiO_2 NTs (system 1). Reaction conditions: water/methanol, proportion 8/1 (v/v).

Conclusions

In summary, a novel route for the growth of TiO_2 nanotube arrays and simultaneous gold NPs impregnation was presented. Au-impregnated TiO_2 NTs annealed at 400 °C led to 100% of anatase phase in all the Au concentrations studied. UV-Vis spectroscopy analyses confirmed that Au NPs were present in the Au-impregnated NT arrays. Stable hydrogen evolution rate was observed with all the NTs used. The presence of Au increased by *ca*. 30% the evolution of hydrogen compared to NTs with 100% anatase phase under the same illumination conditions. In addition, high Au concentrations on the NTs surface region were found. The decrease in the Au NPs concentration has a direct impact on the increase of the hydrogen evolution rate in the water-splitting reaction.

Supplementary Information

Supplementary data (photographs of Au NP colloids before and after dilution with ETG/NH_4F electrolytes, Figure S1) are available free of charge at http://jbcs.sbq.org.br, as a PDF file.

Acknowledgments

This work was partially supported by the Brazilian agencies CNPq, MCT and CAPES. We wish to thank the LNLS staff for the technical support with the GIXRD measurements on the XRD2 Line. We also thank the members of the ion implantation group at the IF-UFRGS.

References

1. Ni, M.; Leung, M. K. H.; Leung, D. Y. C.; Sumathy, K.; *Ren. Sust. Energ. Rev.* **2007**, *11*, 401.
2. Fujishima, A.; Honda, K.; *Nature* **1972**, *238*, 37.
3. Augustynski, J.; *Electrochim. Acta* **1993**, *38*, 43.
4. Chen, X.; Mao, S. S.; *Chem. Rev.* **2007**, *107*, 2891.
5. Mor, G. K.; Carvalho, M. A.; Varghese, O. K.; Pishko, M. V.; Grimes, C. A.; *J. Mater. Res.* **2004**, *19*, 628.
6. Fang, D.; Huang, K. L.; Liu, S. Q.; Huang, J. H.; *J. Braz. Chem. Soc.* **2008**, *19*, 1059.
7. Zhu, K.; Neale, N. R.; Miedaner, A.; Frank, A. J.; *Nano Lett.* **2007**, *7*, 69.

8. Viana, B. C.; Ferreira, O. P.; Souza Filho, A. G.; Mendes Filho, J.; Alves, O. L.; *J. Braz. Chem. Soc.* **2009**, *20*, 167.
9. Bavykin, D. V.; Friedrich, J. M.; Walsh, F. C.; *Adv. Mater.* **2006**, *18*, 2807.
10. Anpo, M.; Shima, T.; Kodama, S.; Kubokawa, Y.; *J. Phys. Chem.* **1987**, *91*, 4305.
11. Thompson, T. L.; Yates, J. T.; *Chem. Rev.* **2006**, *106*, 4428.
12. Serpone, N.; Borgarello, E.; Gratzel, M.; *J. Chem. Soc., Chem. Commun.* **1984**, 342.
13. Duonghong, D.; Borgarello, E.; Gratzel, M.; *J. Am. Chem. Soc.* **1981**, *103*, 4685.
14. Bahnemann, D. W.; Monig, J.; Chapman, R.; *J. Phys. Chem.* **1987**, *91*, 3782.
15. Ruan, C.; Paulose, M.; Varghese, O. K.; Grimes, C. A.; *Sol. Energy Mater.* **2006**, *90*, 1283.
16. Mohapatra, S. K.; Misra, M.; Mahajan, V. K.; Raja, K. S.; *J. Phys. Chem. C* **2007**, *111*, 8677.
17. Vitiello, R. P.; Macak, J. M.; Ghicov, A.; Tsuchiya, H.; Dick, L. F. P.; Schmuki, P.; *Electrochem. Commun.* **2006**, *8*, 544.
18. Mor, G. K.; Prakasam, H. E.; Varghese, O. K.; Shankar, K.; Grimes, C. A.; *Nano Lett.* **2007**, *7*, 2356.
19. Mor, G. K.; Varghese, O. K.; Wilke, R. H. T.; Sharma, S.; Shankar, K.; Latempa, T. J.; Choi, K.-S.; Grimes, C. A.; *Nano Lett.* **2008**, *8*, 1906.
20. Ghicov, A.; Macak, J. M.; Tsuchiya, H.; Kunze, J.; Haeublein, V.; Frey, L.; Schmuki, P.; *Nano Lett.* **2006**, *6*, 1080.
21. Ghicov, A.; Schmidt, B.; Kunze, J.; Schmuki, P.; *Chem. Phys. Lett.* **2007**, *433*, 323.
22. Macak, J. M.; Schmidt-Stein, F.; Schmuki, P.; *Electrochem. Commun.* **2007**, *9*, 1783.
23. Kongkanand, A.; Tvrdy, K.; Takechi, K.; Kuno, M.; Kamat, P. V.; *J. Am. Chem. Soc.* **2008**, *130*, 4007.
24. Turkevich, J.; Stevenson, P. C.; Hillier, J.; *Disc. Farad. Soc.* **1951**, 55.
25. Mohapatra, S. K.; Mahajan, V. K.; Misra, M.; *Nanotechnology* **2007**, *18*, 445705.
26. Macak, J. M.; Tsuchiya, H.; Ghicov, A.; Yasuda, K.; Hahn, R.; Bauer, S.; Schmuki, P.; *Cur. Opin. Solid-State Mater. Sci.* **2007**, *11*, 3.
27. Weitz, D. A.; Lin, M. Y.; Sandroff, C. J.; *Surf. Sci.* **1985**, *158*, 147.
28. Iwase, A.; Kato, H.; Kudo, A.; *Catal. Lett.* **2006**, *108*, 6.
29. Kiwi, J.; Gratzel, M.; *J. Phys. Chem.* **1984**, *88*, 1302.

Received: November 11, 2009
Web Release Date: May 4, 2010